Pressure-velocity coupling for unsteady low Mach number flow simulations: An improvement of the AUSM + -up scheme

Yann Moguen, Erik Dick, Jan Vierendeels, Pascal Bruel

Pressure-velocity coupling for unsteady low Mach number flow simulations: an improvement of the AUSM$^+$-up scheme

Yann Moguen [a], Erik Dick [a,*], Jan Vierendeels [a] and Pascal Bruel [b]

[a] *Ghent University – Department of Flow, Heat and Combustion Mechanics*
Sint-Pietersnieuwstraat, 41 - 9 000 Gent (Belgium)

[b] *CNRS, Laboratoire de Mathématiques et de leurs Applications and Inria CAGIRE Team,*
Université de Pau et des Pays de l'Adour
IPRA, Avenue de l'Université, 64 013 Pau (France)

Abstract

The proper scaling of the pressure-velocity coupling that arises from the Momentum Interpolation approach for unsteady calculation in low Mach number flow is first identified. Then, it is used to suggest a modification of the AUSM$^+$-up scheme that allows acoustic simulations in low Mach number flow.

Key words: Pressure-velocity coupling, Momentum interpolation method, AUSM schemes, Low Mach number flow, Pressure correction, Acoustics

1 Introduction

Unsteady flow calculation in the low Mach number regime, in particular when acoustics has to be accounted for, remains a challenging problem. Usually, the numerical pressure dissipation, necessary to overcome the checkerboard decoupling that arises when a finite volume method in co-located arrangement is applied, is designed from analysis of steady flow problems only. The resulting numerical dissipation is not time-step dependent and therefore cannot permit to properly follow the flow unsteadiness. In Ref. [1], the present authors demonstrated that with a time-consistent definition of the face velocity based on Momentum Interpolation, an accurate representation of travelling acoustic waves is obtained in a low Mach

* Corresponding author. Tel.: +32 9 264 33 01.
Email address: Erik.Dick@Ugent.be (Erik Dick).

number flow [1] . It was also demonstrated that the quite commonly used AUSM$^+$-up definition of the face velocity leads to strong damping of acoustic travelling waves. In the present contribution, we analyse the low Mach number scaling of the pressure dissipation term in the Momentum Interpolation method with the approach of Venkateswaran and Merkle in Refs. [3,4], and derive from it a guideline for improving the pressure dissipation term of the AUSM$^+$-up method. It is demonstrated that the modified AUSM$^+$-up method works very well for some kinds of problems with acoustic waves in low Mach number flow, but that for other types of problems the quality of the Momentum Interpolation can still not be reached.

2 Algorithmic framework

A one-dimensional flow of air in a pipe with variable cross-section area S is considered. The viscous effects and heat transfer are neglected. The flow is governed by the Euler equations,

$$\partial_t(\varrho S) + \partial_x(\varrho v S) = 0, \tag{1}$$

$$\partial_t(\varrho v S) + \partial_x(\varrho v^2 S) + S\partial_x p = 0, \tag{2}$$

$$\partial_t(\varrho E S) + \partial_x(\varrho H v S) = 0, \tag{3}$$

$$\text{with } \varrho e = \frac{1}{\gamma - 1} p \text{ (ideal gas)}, E = e + \frac{1}{2}v^2, \varrho H = \varrho E + p, \tag{4}$$

where t, ϱ, p, v, e, E and H denote time, density, pressure, velocity, internal energy, total energy and total enthalpy per unit mass and x denotes the coordinate in the flow direction. Furthermore, γ is the ratio of the specific heats. The pipe is divided into N cells of equal length Δx. A finite volume formulation is applied, with co-located variables at the centres of the cells. In the convective flux terms in Eqs. (1)-(3), density ϱ, momentum ϱv and total enthalpy per unit of volume ϱH are considered as transported quantities and defined with a second order TVD upwind method. The common velocity in the convective fluxes is considered as the transporting velocity, defined on faces of the cells. With the basic algorithm, the face velocity follows from Momentum Interpolation, as detailed in the next section. The AUSM$^+$-up definition is briefly recalled in a later section. The discretization of the pressure gradient in the momentum equation (2) which requires the definition of the pressure on the cell faces, is also detailed in the next section.

[1] In Ref. [2], we showed that the lack of time consistency of the time-step dependent face velocity influences in a negative way the quality of the solution also for steady flow calculations.

3 Predictor-corrector formulation with face velocity from Momentum Interpolation

In Ref. [1], the present authors formulated a predictor-corrector algorithm of a quite general form. The purpose was to set up a framework for study of a broad class of algorithms. In practice though, such a general formulation is often not necessary. In this paper, we use a predictor-corrector algorithm of classic form, which is a simplified version of the algorithm described in Ref. [1], but with exactly the same result for the problems under study here. Each time-step $n \rightarrow n+1$ is decomposed into a predictor step determining variables at an intermediate level denoted by $\star$, followed by a corrector step with correction quantities denoted by $\prime$. Furthermore, since the equations are non-linear, iterations denoted by k are used in between the time levels n and $n+1$. At the first iteration, variables at level k are equal to those at time level n. At time level n, all nodal quantities are known, as well as the values of the transporting velocity $v^n_{i+1/2}$ and the pressure $p^n_{i+1/2}$ on the faces. The faces are denoted by half indices. The velocity written with subscript $i+1/2$ is the transporting velocity. The velocity as transported quantity is part of the transported momentum and is defined with a TVD upwind method. Distinction between the two meanings of the velocity will always be clear in the formulae.

Predicted values are derived from the continuity equation (1) and the momentum equation (2) by

$$\frac{S_i}{2\tau}(3\varrho^\star_i - 4\varrho^n_i + \varrho^{n-1}_i) + S_{i+1/2}\{\varrho^\star_i + \frac{1}{2}\psi_i(\varrho^k)(\varrho^k_i - \varrho^k_{i-1})\}v^k_{i+1/2} - S_{i-1/2}\{\varrho^\star_{i-1} + \frac{1}{2}\psi_{i-1}(\varrho^k)(\varrho^k_{i-1} - \varrho^k_{i-2})\}v^k_{i-1/2} = 0, \quad (5)$$

$$\begin{aligned}&\frac{S_i}{2\tau}[3(\varrho v)^\star_i - 4(\varrho v)^n_i + (\varrho v)^{n-1}_i] \\ &+ S_{i+1/2}\{(\varrho v)^\star_i + \frac{1}{2}\psi_i((\varrho v)^k)[(\varrho v)^k_i - (\varrho v)^k_{i-1}]\}v^k_{i+1/2} \\ &- S_{i-1/2}\{(\varrho v)^\star_{i-1} + \frac{1}{2}\psi_{i-1}((\varrho v)^k)[(\varrho v)^k_{i-1} - (\varrho v)^k_{i-2}]\}v^k_{i-1/2} \\ &+ S_i(p^k_{i+1/2} - p^k_{i-1/2}) = 0. \quad (6)\end{aligned}$$

The time integration is second order backward. The space discretization is second order upwind TVD, where ψ denotes the limiter function. The parameter τ stands formally for $\Delta t/\Delta x$ and is determined in practice by $\mathrm{CFL}_v/v_{\max}$, where CFL_v denotes a chosen convective CFL number and $v_{\max}$ is the maximum value of the convective velocity in the field. In the numerical tests, only flows with positive convective velocity are considered. Positive values are assumed for the space discretization of the convective terms in Eqs. (5)-(6). Due to the implicit time discretization, the convective CFL number is allowed to be larger than unity. For ac-

curacy reasons, however, we will choose this number much smaller than unity in the tests detailed in later sections.

From the predicted values of density $\varrho_i^\star$ and momentum $(\varrho v)_i^\star$, predicted values of velocity $v_i^\star$ are determined at the nodes. Combined with $p^\star = p^k$, predicted values $e_i^\star$, $E_i^\star$ and $(\varrho H)_i^\star$ are obtained according to Eqs. (4). Next, predicted values of the face quantities $p_{i+1/2}^\star$ and $v_{i+1/2}^\star$ are calculated. The face value of pressure is taken through the low Mach number adaptation of AUSM$^+$ [5], with the scaling function of the AUSM$^+$-up scheme [6], but without the velocity diffusion term in the pressure interpolation formula and without the pressure dissipation term in the definition of the Mach number on the face. For details, we refer to the original publications on the AUSM discretization [5,6], as well as to our earlier publication [1]. This means that the face pressure is determined by a polynomial interpolation between values on both sides of the face, obtained from the TVD definition,

$$p_{i+1/2} = f_p^+(M_{\rm L})p_{\rm L} + f_p^-(M_{\rm R})p_{\rm R}, \tag{7}$$

where the polynomials (f_p^+ and f_p^-) are function of the Mach number on both sides, with a quite particular definition of these Mach numbers, based on a common interface speed of sound.

The Momentum Interpolation technique is based on the observation that the momentum equation (6) at a node is of the form

$$B_i = A_i(\varrho v)_i^\star + \frac{1}{2\tau}[3(\varrho v)_i^\star - 4(\varrho v)_i^n + (\varrho v)_i^{n-1}] + p_{i+1/2}^k - p_{i-1/2}^k, \tag{8}$$

with

$$\begin{aligned} B_i = &-\frac{S_{i+1/2}}{S_i}\{\frac{1}{2}\psi_i((\varrho v)^k)[(\varrho v)_i^k - (\varrho v)_{i-1}^k]\}v_{i+1/2}^k \\ &+ \frac{S_{i-1/2}}{S_i}\{(\varrho v)_{i-1}^\star + \frac{1}{2}\psi_{i-1}((\varrho v)^k)[(\varrho v)_{i-1}^k - (\varrho v)_{i-2}^k]\}v_{i-1/2}^k \end{aligned}$$

and $A_i = \frac{S_{i+1/2}}{S_i}v_{i+1/2}^k$.

A similar equation is postulated for the momentum terms on a face as

$$B_{i+1/2} = A_{i+1/2}(\varrho v)_{i+1/2}^\star + \frac{1}{2\tau}[3(\varrho v)_{i+1/2}^\star - 4(\varrho v)_{i+1/2}^n + (\varrho v)_{i+1/2}^{n-1}] + p_{i+1}^k - p_i^k, \tag{9}$$

where two terms in the balance of the momentum fluxes are interpolated, but where the inertia term and the pressure term are written directly on the face. We use the so-called classic Rhie-Chow interpolation, namely:

$$\frac{2}{A_{i+1/2}} = \frac{1}{A_i} + \frac{1}{A_{i+1}}, \frac{B_{i+1/2}}{A_{i+1/2}} = \frac{B_i}{A_i} + \frac{B_{i+1}}{A_{i+1}},$$

but the precise way of interpolation is not critical [1,7,8]. The transporting face velocity is deduced from the momentum equation by

$$v^{\star}_{i+1/2} = (\varrho v)^{\star}_{i+1/2} / \varrho^{\star}_{i+1/2}, \tag{10}$$

where the face density is defined with the TVD upwind method.

Corrections for the pressure are derived from the energy equation. This equation is discretized in the same style as the continuity equation and the momentum equation by

$$\begin{aligned}
&\frac{S_i}{2\tau}[3(\varrho E)^{\star}_i + 3(\varrho E)'_i - 4(\varrho E)^n_i + (\varrho E)^{n-1}_i] \\
&+ S_{i+1/2}\{(\varrho H)^{\star}_i + \frac{1}{2}\psi_i((\varrho H)^{\star})[(\varrho H)^{\star}_i - (\varrho H)^{\star}_{i-1}]\} v^{\star}_{i+1/2} \\
&- S_{i-1/2}\{(\varrho H)^{\star}_{i-1} + \frac{1}{2}\psi_{i-1}((\varrho H)^{\star})[(\varrho H)^{\star}_{i-1} - (\varrho H)^{\star}_{i-2}]\} v^{\star}_{i-1/2} \\
&\qquad + S_{i+1/2}(\varrho H v)'_{i+1/2} - S_{i-1/2}(\varrho H v)'_{i-1/2} = 0.
\end{aligned} \tag{11}$$

The corrections on the enthalpy flux terms are written as

$$(\varrho H v)'_{i+1/2} = H^{\star}_{i+1/2}(\varrho v)'_{i+1/2} + (\varrho H)'_{i+1/2} v^{\star}_{i+1/2}, \tag{12}$$

with $H^{\star}_{i+1/2} = (\varrho H)^{\star}_{i+1/2} / \varrho^{\star}_{i+1/2}$, where both terms in the ratio are defined with the TVD upwind method.

Neglecting the contribution of the kinetic energy, the corrections for total energy and total enthalpy are written as

$$(\varrho E)'_i = \frac{1}{\gamma - 1} p'_i, (\varrho H)'_{i+1/2} = \frac{\gamma}{\gamma - 1} p'_{i+1/2}, \tag{13}$$

where $p'_{i+1/2}$ is interpolated with the AUSM$^+$-up polynomials as

$$p'_{i+1/2} = f^+_p(M^{\star}_i) p'_i + f^-_p(M^{\star}_{i+1}) p'_{i+1}. \tag{14}$$

The momentum corrections are written in SIMPLE-style, based on the momentum equations (8) and (9), as

$$(A_i + \frac{3}{2\tau})(\varrho v)'_i = -(p'_{i+1/2} - p'_{i-1/2}), \tag{15}$$

$$(A_{i+1/2} + \frac{3}{2\tau})(\varrho v)'_{i+1/2} = -(p'_{i+1} - p'_i). \tag{16}$$

Substitution of (13), (14) and (16) into (12) and (11) leads to an extended Poisson equation for the pressure corrections. This equation is solved by a Gaussian elimination procedure. The pressure corrections are then further used to determine

the corrections of the momentum values at the nodes and on the faces by (15) and (16). Density is corrected by $\varrho_i' = (\partial_p \varrho)_i^\star p_i'$. The whole procedure is then repeated until convergence. This results then in the equations (5), (6) and (11) with values at the $*-$level and $k-$level replaced by values at the time level $n+1$ and correction values in (11) equal to zero. These equations are discretized in the same way and use the same value of the transporting velocity on the faces.

4 Transporting velocity in Momentum Interpolation

The scaling property of the transporting velocity that arises in the Momentum Interpolation approach is studied, along with its relation with the time-step independency of the steady state, which is related to the time consistency of the scheme.

4.1 Scaling property

We introduce a reference length l_r, pressure p_r, density ϱ_r, velocity v_r and time t_r. Our purpose is to study acoustic propagation in low Mach number flow. Therefore, we choose the length of the flow domain as reference length, the convective velocity v_r of the background low Mach number flow and the velocity $\sqrt{p_\mathrm{r}/\varrho_\mathrm{r}}$, which is of the same order as the velocity of sound in the mean flow, as reference velocities. The reference Mach number is thus defined as $\mathrm{M} = v_\mathrm{r}/\sqrt{p_\mathrm{r}/\varrho_\mathrm{r}}$. The reference time is of the order of the time needed by an acoustic wave to travel through the reference length, thus $t_\mathrm{r} = l_\mathrm{r}/\sqrt{p_\mathrm{r}/\varrho_\mathrm{r}}$. The non-dimensional form of the discretized momentum equation becomes

$$B_i = A_i(\varrho v)_i^\star + \frac{1}{\mathrm{M}^2}(p_{i+1/2}^k - p_{i-1/2}^k) - \frac{2\mathrm{S_t}}{\tau}(\varrho v)_i^n + \frac{\mathrm{S_t}}{2\tau}(\varrho v)_i^{n-1} + \frac{3\mathrm{S_t}}{2\tau}(\varrho v)_i^\star \quad (17)$$

where all parameters are non-dimensional, A_i and B_i belong to $\mathcal{O}(1)$, and where $\mathrm{S_t} = (l_\mathrm{r}/v_\mathrm{r})/t_\mathrm{r}$ is the reference Strouhal number. The non-dimensional form of the face velocity equation (9) is similarly

$$(\varrho v)_{i+1/2}^\star = K_C B_{i+1/2} - K_P(p_{i+1}^k - p_i^k) + K_I[2\varrho_{i+1/2}^n v_{i+1/2}^n - \frac{1}{2}\varrho_{i+1/2}^{n-1} v_{i+1/2}^{n-1}], \quad (18)$$

where

$$K_C = (A_{i+1/2} + \frac{3\mathrm{S_t}}{2\tau})^{-1}, K_P = \frac{K_C}{\mathrm{M}^2}, K_I = K_C\frac{\mathrm{S_t}}{\tau} \quad (19)$$

are the coefficients of the convection, pressure and inertia terms.

For acoustic problems in low Mach number flow, the reference time is $t_\mathrm{r} = \mathrm{M}l_\mathrm{r}/v_\mathrm{r}$ (*cf. e.g.* Ref. [4]), so that the reference Strouhal number $\mathrm{S_t}$ belongs to $\mathcal{O}(1/\mathrm{M})$.

Table 1
Scalings of the face velocity coefficients for low Mach number acoustic problems with Momentum Interpolation

Convection term	Pressure term	Inertia term	Time consistency
$(1+\frac{1}{\tau \mathrm{M}})^{-1}$	$(\mathrm{M}^2+\frac{\mathrm{M}}{\tau})^{-1}$	$(1+\tau \mathrm{M})^{-1}$	yes

Thus, the scaling behaviour of the coefficients (19) can be expressed in terms of τ and M only. The results are given in Table 1. Let us emphasize that these scaling properties are the same as in the discretized momentum equation (17).

4.2 Time consistency

As pointed out by Pascau [8], an important property, which is related to the time consistency of the scheme, is the time-step independency of the transporting velocity if a steady state is reached. Inspection of Eq. (18) with coefficients (19), shows that, at steady state ($n = n-1 = \star$), the transporting velocity at the face is independent of the time-step. Further, the correct M^2 scaling of the convection term with respect to the pressure coefficient in unsteady flows (see Table 1) is maintained for steady flows.

Physically, at low Mach number, the momentum equation (17) becomes a balance between the pressure term and the inertia term. Such a balance is also expressed locally on the face of a control volume by Eq. (18). We say that the scheme is time-consistent since the individual terms in the expression (18) are similar to corresponding terms in the momentum equation at the nodes (17).

5 Transporting velocity in AUSM$^+$-type schemes

The idea developed in this section is that the previous observations concerning the scaling property of the transporting velocity obtained through the Momentum Interpolation method can be applied with advantage to Godunov-type schemes. As an example of such schemes, AUSM$^+$-up is considered [6]. Then, variants of AUSM$^+$-up adapted for unsteady calculations are studied.

5.1 Necessity of a time-step dependent definition of the transporting velocity

Possible checkerboard decoupling of the pressure is avoided in the AUSM$^+$-up scheme by adding a pressure dissipation term in the interpolation formula for the

face velocity. First, the interface Mach number is written as

$$M_{i+1/2} = f_M^+(M_{\rm L}) + f_M^-(M_{\rm R}) - \frac{k_p}{f(M_{0,i+1/2})} \max\{1-(\overline{M}_{i+1/2})^2\sigma, 0\} \, \frac{p_{\rm R}-p_{\rm L}}{\varrho_{i+1/2} c_{i+1/2}^2}, \tag{20}$$

where the expressions for $f_M^{\pm}$, k_p, σ, $\overline{M}_{i+1/2}$, $M_{0,i+1/2}$, $c_{i+1/2}$ and f are given in Ref. [6], and $\varrho_{i+1/2} = (\varrho_{\rm L} + \varrho_{\rm R})/2$. Notice that the interpolation polynomials $f_M^{\pm}$ are different from $f_p^{\pm}$ in Eqs. (7) and (14).

The face velocity is defined by

$$v_{i+1/2} = c_{i+1/2} M_{i+1/2}. \tag{21}$$

We remark that we may replace the face velocity from Momentum Interpolation (9) by (21) and still use the pressure correction algorithm, but now with (15) replaced by

$$(\varrho v)'_i = -\kappa_{i+1/2}(p'_{i+1} - p'_i), \tag{22}$$

with

$$\kappa_{i+1/2} = \frac{k_p}{f(M^\star_{0,i+1/2})} \max\{1-(\overline{M}^\star_{i+1/2})^2\sigma, 0\} \frac{\varrho^\star_L}{\varrho^\star_{i+1/2} c^\star_{i+1/2}}.$$

The expression (22) has the correct Mach number scaling for steady flows, but misses the time-dependent term of the Momentum Interpolation approach (*cf.* Table 1).

The effect of the inappropriate pressure dissipation of AUSM$^+$-up for acoustic simulation in low Mach number flow was evidenced in our previous study [1]. As it is illustrated in Fig. 1, which presents results extracted from [1], the AUSM$^+$-up scheme leads to unphysical dissipation of acoustic travelling waves when compared to the results obtained with the Momentum Interpolation method. Thus, it can be hoped that better results be obtained with a modified form of AUSM$^+$-up, in order to recover the time-step dependency and the scaling property of the pressure-velocity coupling of the Momentum Interpolation method.

5.2 Time-step dependent AUSM$^+$-type interpolation

A modification of AUSM$^+$-up that satisfies the time-step dependency as well as the suitable scaling property of the pressure-velocity coupling evidenced in Sec. 4, is suggested. It is compared with the LDFSS-2001 scheme described in Ref. [9], which is an AUSM variant involving an explicit time-step dependency as well.

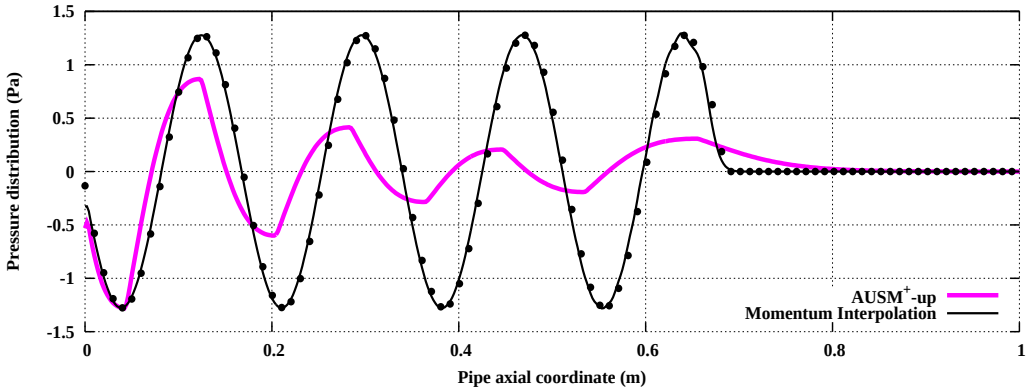

Fig. 1. Downstream propagation of a wave forced at the left boundary of a pipe of constant cross-section area S. Pressure distribution at $t = 2$ ms. The inlet velocity is specified to oscillate about a mean value V, as $v^{\dagger}(t) = V[1 + A\sin(2\pi f t)]$, where $A = 10^{-2}$, $V = 0.30886$ ms^{-1} and $f = 2\ 10^3$ Hz. Exact solution: • (linear acoustics). Number of cells: $N = 500$. Mach number of the background flow: $\mathrm{M} = 10^{-3}$. Convective CFL number: $\mathrm{CFL}_v = 10^{-4}$. TVD-limiter is Bounded Central (Figure adapted from Ref. [1]).

• MODIFIED AUSM$^+$-up. To adapt the AUSM$^+$-up scheme in order to obtain a transporting velocity suitable for acoustic simulation in low Mach number flows, the interface Mach number given by Eq. (20) is modified such that the scaling of the coefficient of the pressure gradient becomes $(\mathrm{M}^2 + \mathrm{M}/\tau)^{-1}$ in acoustic regime, as for the Momentum Interpolation approach (see Table 1):

$$M_{i+1/2} = f_M^+(M_\mathrm{L}) + f_M^-(M_\mathrm{R}) - k_p \max\{1 - (\overline{M}_{i+1/2})^2\sigma, 0\} \frac{p_\mathrm{R} - p_\mathrm{L}}{\varrho_{i+1/2} c_{i+1/2}[f(M_{0,i+1/2})c_{i+1/2} + \frac{\beta}{\tau}]}, \quad (23)$$

where $\beta \in \mathcal{O}(1)$. To verify the correct scaling, the reference quantities of Sec. 4.1 are used for the non-dimensionalization of the pressure gradient term in Eq. (23). As $k_p \max\{1 - (\overline{M}_{i+1/2})^2\sigma, 0\} \in \mathcal{O}(1)$ if $\mathrm{M} \ll 1$, it is sufficient to note that the ratio in the last term of Eq. (23) is not modified in non-dimensional form. Notice that in Eq. (22), κ is then given by

$$\kappa_{i+1/2} = k_p \max\{1 - (\overline{M}^\star_{i+1/2})^2\sigma, 0\} \frac{\varrho^\star_\mathrm{L}}{\varrho^\star_{i+1/2}[f(M^\star_{0,i+1/2})c^\star_{i+1/2} + \frac{\beta}{\tau}]}.$$

• LDFSS-2001. A simplified version of the transporting velocity of LDFSS-2001 described in Ref. [9], in order to bring it in the form (23), is

$$v_{i+1/2} = \tilde{c}_{i+1/2,\mathrm{conv}} \left(M_\mathrm{L}^+ + M_\mathrm{R}^- - \tilde{M}_{i+1/2} \frac{p_\mathrm{R} - p_\mathrm{L}}{\varrho_{i+1/2} v^2_{1/2,\mathrm{ref,conv}}} \right), \quad (24)$$

where

$$v^2_{1/2,\mathrm{ref},\mathrm{conv}} = \max\{\tau^{-2}, |v_i|^2_{\max}\},\ \varrho_{i+1/2} = \frac{1}{2}(\varrho_\mathrm{L} + \varrho_\mathrm{R}),$$

$$\tilde{c}_{i+1/2,\mathrm{conv}} = \sqrt{v^2_{i+1/2} + 4v^2_{1/2,\mathrm{ref},\mathrm{conv}}},\ v_{i+1/2} = \frac{1}{2}(v_\mathrm{L} + v_\mathrm{R}),$$

$$M^{\pm}_{\mathrm{L/R}} = \pm\frac{1}{4}(M_{\mathrm{L/R}} \pm 1)^2,\ M_{\mathrm{L/R}} = \frac{v_{\mathrm{L/R}}}{\tilde{c}_{i+1/2,\mathrm{conv}}},$$

$$\tilde{M}_{i+1/2} = \frac{1}{2}[M^+_\mathrm{L} - \frac{1}{2}(M_\mathrm{L} + |M_\mathrm{L}|) - M^-_\mathrm{R} + \frac{1}{2}(M_\mathrm{R} - |M_\mathrm{R}|)].$$

In Eq. (22), κ is given by

$$\kappa_{i+1/2} = \frac{\tilde{c}_{i+1/2,\mathrm{conv}}\tilde{M}_{i+1/2}}{v^2_{1/2,\mathrm{ref},\mathrm{conv}}}.$$

Notice that the transporting velocity definition given in Ref. [9] needs to be simplified in the present paper, in order to obtain an expression that does not involve the transported quantities. The algorithm described in Sec. 2 can then be used without modification. Using the same reference quantities as for the scaling study of the modified AUSM$^+$-up scheme, the non-dimensional pressure gradient term in Eq. (24), at the leading order in the power of the reference Mach number, is

$$v_\mathrm{r}\,\frac{p_\mathrm{R} - p_\mathrm{L}}{\varrho_{i+1/2}\frac{\mathrm{M}}{\tau}}.$$

Thus, LDFSS-2001 has the proper *unsteady* low Mach number scaling, for very low Mach number. However, the scaling is not exactly the same as the one of the properly scaled Momentum Interpolation methods considered in Sec. 4 (*cf.* Refs. [7,8]), which is mimicked by the modified AUSM$^+$-up defined before. Further, both the modified AUSM$^+$-up scheme and the LDFSS-2001 scheme lack an inertia term in the face velocity definition.

6 Numerical experiments

Two test cases of increasing complexity are now considered to test the proposed modified AUSM$^+$-up scheme. They differ essentially by the spectral content of the propagating acoustic wave. For both test cases, boundary conditions are not relevant because we do not continue the calculations until waves reach boundaries. For test case 1 used previously to illustrate the deficiency of AUSM$^+$-up (Fig. 1), the improvement by the modified scheme is impressive. As shown in Fig. 2, both the LDFSS-2001 and the modified schemes permit to simulate accurately the propagation of the harmonic wave. For propagation of a non-harmonic wave (pulse), the

results differ more. On a propagation distance less than one meter, both the modified AUSM$^+$-up and LDFSS-2001 schemes give quite good results with only a slight difference of the pulse when compared to the Momentum Interpolation results (Fig. 3, a-b). Note that in such a case, the results by the standard AUSM$^+$-up scheme are of very bad quality. If a longer distance of propagation is considered (Fig. 3, c-d), the Momentum Interpolation method outperforms both the modified AUSM$^+$-up and LDFSS-2001 schemes. The reason is the lack of the inertia term in the face velocity definition, necessary for full time consistency of the face velocity. The lack of the inertia term has as consequence that the quality of the results varies with the value of the coefficient β and that its optimum value is problem dependent. For the case shown in Fig. 2, the best results are obtained for $\beta = 1$, while for the case shown in Fig. 3 the best results are obtained for $\beta = 0.01$.

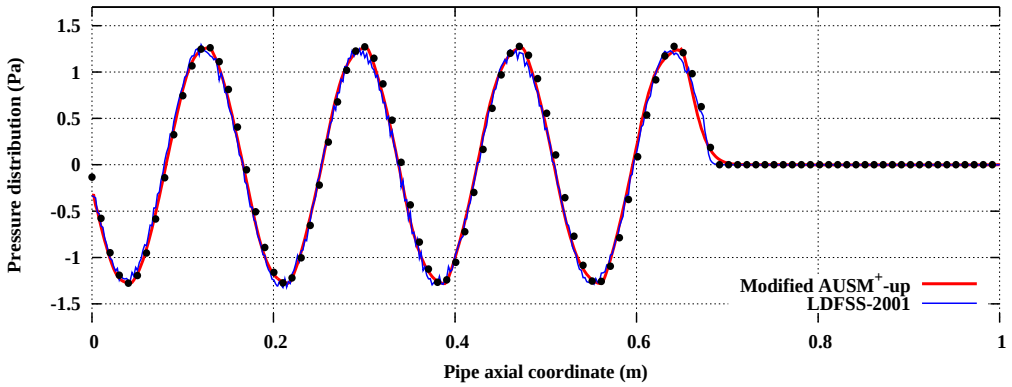

Fig. 2. Downstream propagation of a wave forced at the left boundary of a pipe of constant cross-section area S. Pressure distribution at $t = 2$ ms. Exact solution: • (linear acoustics). Number of cells: $N = 500$. Mach number of the background flow: $\mathrm{M} = 10^{-3}$. Convective CFL number: $\mathrm{CFL}_v = 10^{-4}$.

7 Conclusion

The time-step dependency and the scaling of the pressure-velocity coupling suitable for unsteady calculation in low Mach number flow, including acoustic features, has been identified in the Momentum Interpolation approach suggested in Refs. [7,8]. We observed that the proper form of the inertia term in the transporting velocity definition is related to the time-step independency of the steady state. This suitable scaling of the pressure gradient dissipation has then been used to suggest a modification of AUSM$^+$-up scheme to allow acoustic simulations in low Mach number flow. The accuracy improvement when the solution is compared to the one of the original AUSM$^+$-up scheme indicates that the scaling identified in the Momentum Interpolation approach can be applied with advantage to Godunov-type schemes.

References

[1] Y. Moguen, T. Kousksou, P. Bruel, J. Vierendeels, and E. Dick. Pressure-velocity coupling allowing acoustic calculation in low mach number flow. *J. Comput. Phys.*, 231:5522–5541, 2012.

[2] Y. Moguen, T. Kousksou, P. Bruel, J. Vierendeels, and E. Dick. Rhie-Chow interpolation for low Mach number flow allowing small time steps. In J. Fort, J. Fürst, J. Halama, R. Herbin, and F. Hubert, editors, *Finite Volumes for Complex Applications VI – Problems & Perspectives*, volume 1, pages 703–711, Prague, Czech Republic, June 6-10, Springer 2011.

[3] S. Venkateswaran and C.L. Merkle. The Use of Asymptotic Expansions to Assess the Accuracy of Euler and Navier–Stokes Computations. AIAA Paper No. 99-3266, 1999.

[4] S. Venkateswaran and C.L. Merkle. Efficiency and Accuracy Issues in Contemporary CFD Algorithms. AIAA Paper No. 2000-2251, 2000.

[5] M.-S. Liou. A Sequel to AUSM: AUSM$^+$. *J. Comp. Phys.*, 129:364–382, 1996.

[6] M.-S. Liou. A Sequel to AUSM, part II: AUSM$^+$-up for all speeds. *J. Comp. Phys.*, 214:137–170, 2006.

[7] F.S. Lien and M.A. Leschziner. A general non-orthogonal collocated finite volume algorithm for turbulent flow at all speeds incorporating second-moment turbulence-transport closure, Part 1: Computational implementation. *Comput. Methods Appl. Mech. Engrg.*, 114:123–148, 1994.

[8] A. Pascau. Cell face velocity alternatives in a structured colocated grid for the unsteady Navier-Stokes equations. *Int. J. Numer. Meth. Fluids*, 65:812–833, 2011.

[9] D.A. Cassidy, J.R. Edwards, and M. Tian. An investigation of interface-sharpening schemes for multi-phase mixture flows. *J. Comp. Phys.*, 228:5628–5649, 2009.

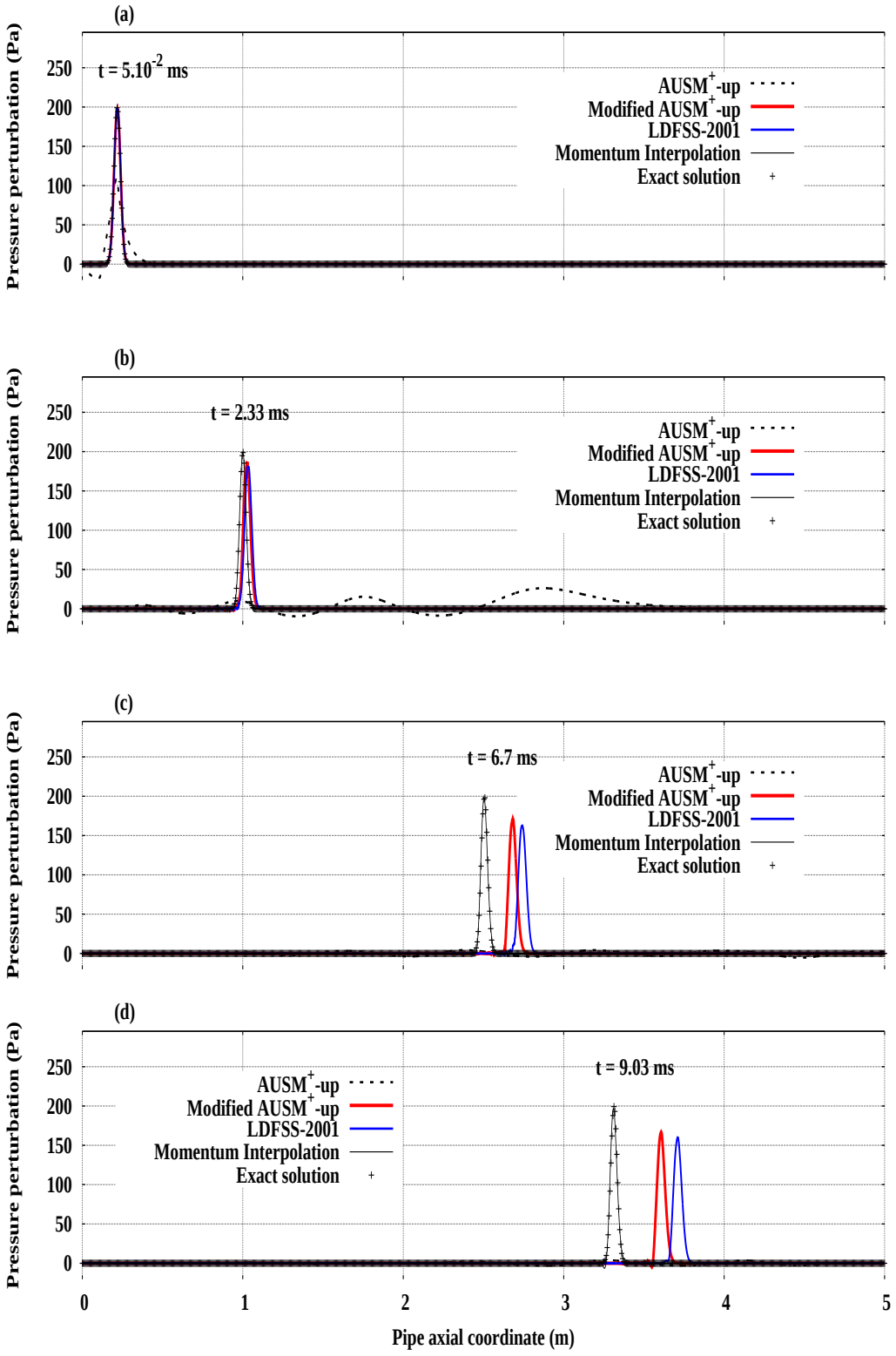

Fig. 3. Downstream propagation of an acoustic pulse in a pipe of constant cross-section area S. Pressure distribution at $t = 5\ 10^{-2}$ ms (top), $t = 2.33$ ms, $t = 6.7$ ms and $t = 9.03$ ms (bottom). Exact solution: linear acoustics. Number of cells: $N = 2\ 500$. Mach number of the background flow: $\mathrm{M} = 10^{-4}$; convective CFL number: $\mathrm{CFL}_v = 5\ 10^{-4}$. Results by AUSM$^+$-up coincide with the coordinate-axis for $t = 6.7$ ms and $t = 9.03$ ms.